

A Self-Replicating Radiation-Shield for Human Deep-Space Exploration: Radiotrophic Fungi can Attenuate Ionizing Radiation aboard the International Space Station

Graham K. Shunk^{1,2*}, Xavier R. Gomez^{1,3}, Nils J. H. Aversch^{4,5*}

¹ Higher Orbits “Go For Launch!” Program

² North Carolina School of Science and Mathematics, Physics Department, Durham NC, United States

³ University of North Carolina at Charlotte, Charlotte, NC, United States

⁴ Center for the Utilization of Biological Engineering in Space

⁵ Department of Civil and Environmental Engineering, Stanford University, Stanford, CA, United States

* To whom correspondence should be directed: <graham1118@gmail.com>,

<nils.aversch@uq.net.au>

Abstract

The greatest hazard for humans on deep-space exploration missions is radiation. To protect astronauts venturing out beyond Earth’s protective magnetosphere and sustain a permanent presence across the solar system, advanced passive radiation protection is highly sought after. Due to the complex nature of space radiation, there is likely no one-size-fits-all solution to this problem, which is further aggravated by up-mass restrictions. In search of innovative radiation-shields, biotechnology appeals with suitability for *in-situ* resource utilization (ISRU), self-regeneration, and adaptability.

Certain fungi thrive in high-radiation environments on Earth, such as the contamination radius of the Chernobyl Nuclear Power Plant. Analogous to photosynthesis, these organisms appear to perform radiosynthesis, utilizing the pigment melanin to harvest gamma-radiation and generate chemical energy. It is hypothesized that the dissipation of radiation by these organisms translates to a radiation shield. Here, growth of *Cladosporium sphaerospermum* and its capability to attenuate ionizing radiation, was studied aboard the International Space Station (ISS) over a period of 30 days, as an analog to habitation on the surface of Mars. At full maturity, radiation beneath a ≈ 1.7 mm thick lawn of the dematiaceous radiotrophic fungus (180° protection radius) was $2.17 \pm 0.25\%$ lower as compared to the negative control. Based on an estimated growth advantage in space of $\sim 20\%$, the reduction of radiation was attributed to the fungus’ radiotropism and melanin-content. This was supported by calculations based on Lambert's law, where the biomass could be approximated to $8.6 \pm 0.9\%$ [w/w]. The analysis of the experimental data was further complemented by an attenuation analysis subject to a Martian radiation environment scenario that put the shielding capacity of melanized (bio)materials into perspective. Compatible with ISRU, bio-based melanin-containing composites are promising as a means for radiation shielding while reducing overall up-mass, as is compulsory for future Mars-missions.

Abbreviations

B, buildup-factor; BoPET, biaxially-oriented polyethylene terephthalate; CDW, cell dry-weight; CPM, counts per minute; CWW, cell wet-weight; DHN, 1,8-dihydroxynaphthalene; GCR, galactic cosmic radiation; HDPE, high-density polyethylene; HZE, high atomic number and energy; ISRU, *in-situ* resource utilization; ISS, international space station; LAC, linear attenuation coefficient; LEO, low earth-orbit; MAC, mass attenuation coefficient; PDA, potato dextrose agar; RT, room temperature.

Keywords: Space, Radiation-Shield, Fungus, *Cladosporium sphaerospermum*, Radiotrophic, ISRU

Introduction

Background

With concrete efforts to return humans to the Moon by 2024 under the Artemis program and establish a permanent foothold on the next rock from Earth by 2028, humankind reaches for Mars as the next big leap in space exploration¹. In preparation for prolonged human exploration missions venturing past Earth-orbit and deeper into space, the required capabilities significantly increase². While advanced transportation solutions led by the private and public sectors alike (Starship, New Glenn, SLS/Orion) are pivotal and have already reached high technological readiness, life support systems as well as crew health and performance capabilities are equally essential. Therefore, any mission scenario such as ‘Design Reference Architecture 5.0’³ or ‘Mars Base Camp’⁴ (with up to 1000 days of crewed usage), must include innovative solutions that can meet the needs and address the hazards of prolonged residence on celestial surfaces⁴.

The foremost threat to the short- and long-term health of astronauts on long-duration deep-space missions is radiation^{5,6}. Over one year, the average person on Earth is dosed with about 6.2 mSv⁷, while the average astronaut on the International Space Station (ISS) is exposed to an equivalent of approximately 144 mSv⁸, and one year into a three-year mission to Mars, an astronaut would already have accumulated some 400 mSv, primarily from Galactic Cosmic Radiation (GCR)⁹. While the particular health effects of interplanetary radiation exposure have still not been fully assessed¹⁰, it is clear that adequate protection against space-radiation is crucial for missions beyond Earth-orbit, but is more than any other factor restricted by up-mass limitations¹¹. Both active and passive radiation-shielding, the latter investigating inorganic as well as organic materials, have been and are extensively studied^{12,13}.

In-Situ Resource Utilization (ISRU) will play an integral role to provide the required capabilities, as well as to break the supply chain from Earth and establish sustainable methods for space exploration because once underway there virtually is no mission-abort scenario¹⁴. For ISRU, biotechnology holds some of the most promising approaches^{15,16,17}, posing useful for providing nutrition¹⁸, producing raw-materials¹⁹ and consumables²⁰, and potentially even “growing” radiation shielding^{21,22}.

Among all domains of life exist extremophiles that live and persist in highly radioactive environments, including bacteria, fungi, as well as higher organisms such as insects^{23,24}. Certain fungi can even utilize ionizing radiation through a process termed radiosynthesis²⁵, analogous to how photosynthetic organisms turn energy from visible light into chemical energy^{26,27}. Large amounts of melanin in the cell walls of these fungi protect the cells from radiation damage while also mediating electron-transfer, thus allowing a net energy gain²⁸. Melanized fungi have been found to thrive in highly radioactive environments such as the cooling ponds of the Chernobyl Nuclear Power Plant²⁷, where radiation levels are three to five orders of magnitude above normal background levels²⁹. Additionally, they populate the interiors of spacecraft in low Earth orbit (LEO), where exposure to ionizing radiation is also intensified²⁷. Black molds and their spores have been found to remain viable even after exposure to several months’ worth of Space radiation (or an equivalent radiation dose)³⁰. How these organisms protect themselves from radiation damage has been the subject of intense study; melanins have also specifically been explored as biotechnological means for radiation shielding^{31,32}.

Here, we explore the opportunity to utilize the dissipation of radiation by melanized fungi as part of a multi-faceted solution to passive radiation-shielding for ISRU^{18,33}. In an additional analysis based on the concept of linear attenuation (Lambert’s law)³⁴, we assess the potential of melanized fungus, as well as the specific contribution of melanin, to provide adequate shielding against cosmic radiation.

Concept

This experiment tested the capability of *Cladosporium sphaerospermum* (a melanized, radiotrophic fungus²¹, cf. supplementary material 1, section A for details) to attenuate ionizing gamma-radiation in space. The preference of *C. sphaerospermum* for environments with extreme radiation-levels on Earth (e.g. Chernobyl) is well documented³⁵. Consequently, it has been hypothesized that similar proliferation occurs in response to the high radiation environment off-Earth and that such melanized fungi can be utilized for radioprotection in Space³². The objective of this experiment was to conduct a proof-of-principle study on a single payload, utilizing basic flight hardware for an autonomous experiment in the unique radiation environment of the ISS. This offers the opportunity to test the fungus' response to, and ability to shield from cosmic radiation.

Materials & Methods

Experimental Setup

Space Tango (Space Tango, Inc., Lexington, KY, USA) was contracted for experimental design and construction (terrestrial logistics and on-orbit operations)³⁶. The initial concept for the experimental design was utilized by Space Tango for assembly of the flight-hardware and implementation aboard the ISS within TangoLab™ facilities. The flight-hardware was housed in a 4"×4"×8" double unit standard-size CubeLab™ hardware module (cf. supplementary material 1, figure S1) and consisted of the following main components: two Raspberry Pi 3 Model B+ (Raspberry Pi Foundation, Caldecote, Cambridgeshire, UK) single-board computers, EP-0104 DockerPi PowerBoard (Adafruit Industries, New York, NY, USA), Pocket Geiger Type5, X100-7 SMD (Radiation Watch, Miyagi, Japan), Raspberry Pi Camera v2 (Raspberry Pi Foundation, Caldecote, Cambridgeshire, UK) and light source (0.8 W LED-strip) for imaging, DHT22 integrated environmental sensor suite (Aosong Electronics Co. Ltd, Huangpu District, Guangzhou, China) for temperature and humidity readings, a real-time WatchDog™ timer (Brentek International Inc., York, PA, USA), and D6F-P0010A1 (Omron Electronics LLC, Hoffman Estates, IL, USA) electronic flow-measurement system. One Raspberry Pi ("auxiliary-computer") running Raspbian v10.18 was dedicated to photography, lighting, temperature, humidity, and electronic flow measurement (EFM) readings, while the second Raspberry Pi ("flight-computer") controlled radiation measurements, stored in a probed Logger Memobox (Fluke Corporation, Everett, WA, USA). The assembled flight-hardware was calibrated and vetted before flight; in particular consistency of the two Geiger counters was confirmed so that no deviation existed between them.

Cladosporium sphaerospermum (ATCC® 11289™) was obtained from Microbiologics (St. Cloud, Minnesota, USA), catalog no. 01254P. Further details on the employed microorganism can be found in supplementary material 1, section A. Growth medium was potato dextrose agar "PDA" from Carolina Biological (Burlington, North Carolina, USA) obtained as "Prepared Media Bottle" (approx. composed of 15 g/L agar, 20 g/L glucose, and 4 g/L starch). A total of 20 mL PDA (dyed with orange 1) was used to fill the two compartments of a split Petri dish (100×15 mm). The agar plate was sealed with parafilm post-inoculation. With a total height of the Petri dish of 15 mm and a 75 cm² surface area, the thickness of the PDA was ~ 13.33 mm, leaving an approx. 1.67 mm gap for the fungal growth layer. Cellular mass density of fungal biomass (1.1 g/cm³)³⁷ was assumed to remain unaffected by microgravity. The hardware was fully assembled before the inoculation of the agar with *C. sphaerospermum* to minimize latent growth of the fungus while in transit. A block-chart of the experimental flight hardware setup is given in figure 1 while further details are provided in supplementary material 1, section B.

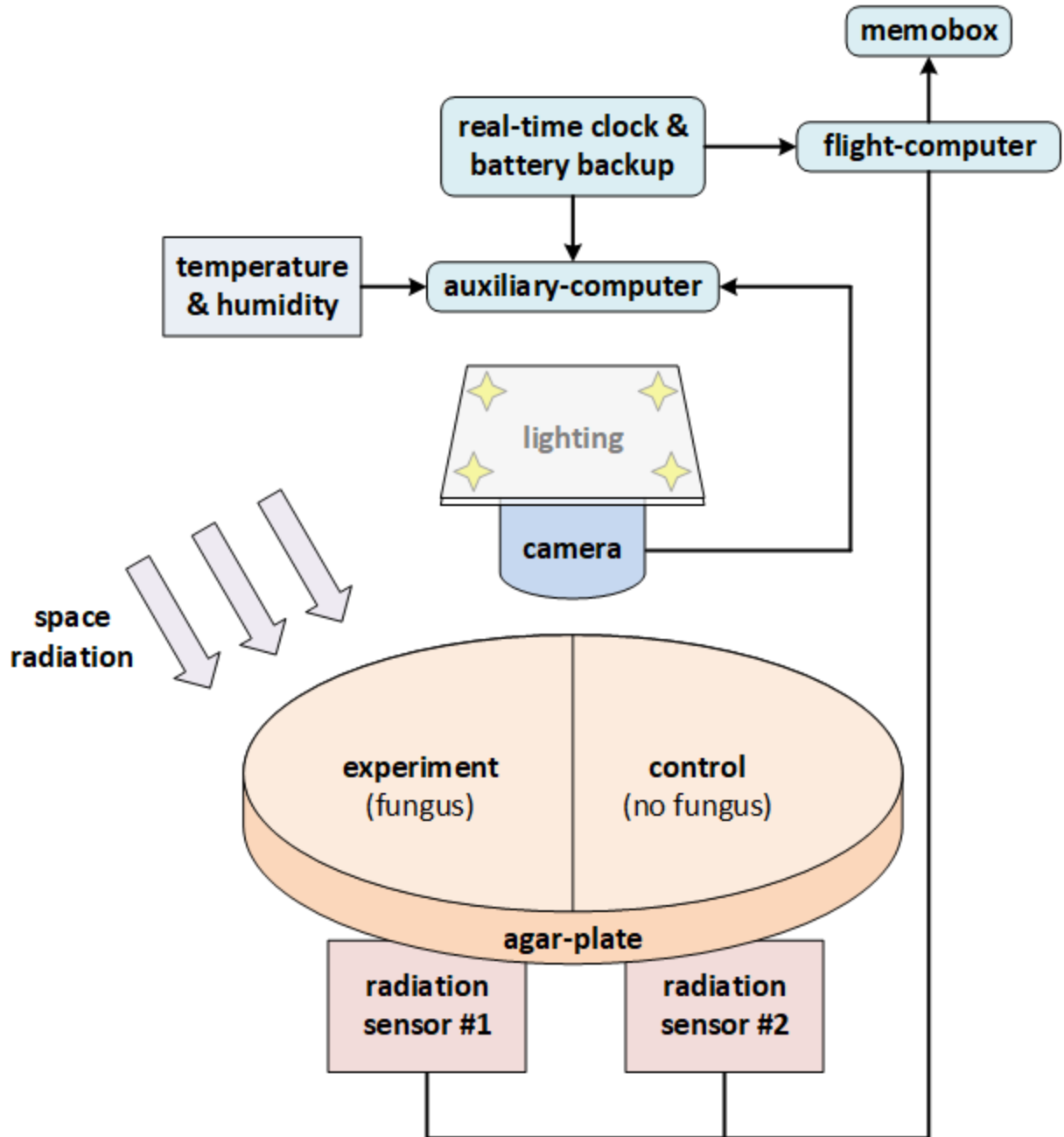


Figure 1: Block-chart of the experimental flight hardware setup. The single (split) Petri dish accommodated both the experiment (agar + fungus), as well as the negative-control (agar only). The two radiation sensors were situated in parallel directly beneath the Petri dish (one for each side). Note that “shielding” is one-sided only (for simplicity of experimental setup) since radiation is ubiquitous in space.

Vetting for Cold-Stow

The response of *Cladosporium sphaerospermum* to cold-storage was determined in a preliminary experiment. A total of six Petri dishes containing PDA were inoculated with the fungus, five were stored at 4°C with one kept at room temperature (RT) as control. Plates were removed sequentially after 1, 5, 10, 15 and 20 days. Fungal growth on each plate was monitored at RT and compared to the control.

On-Orbit Implementation

The equipment was packaged with the inoculated Petri dish before flight, accommodated in a 2U CubeLab™ (Sealed)³⁸, between Dec 2018 and Jan 2019. Lead-time before the launch was 2 days in cold-stow. Transition time to LEO was 69 hours and 20 minutes (time to “power-on” after inoculation), transported to the ISS in cold storage (4°C) on SpaceX mission CRS-16.

On orbit, the experiment was oriented such that the Petri dish and Geiger counters faced away from Earth. Pictures of the Petri dish were taken in 30-minute intervals (as set by the watchdog time) for 576 h, resulting in 1139 images. Temperature, humidity and radiation were measured every ~ 110 seconds throughout the 718 h run-time of the experiment. The three temperature sensors recorded 27772 measurements each. Radiation was measured incrementally; 23607 radiation and noise-counts were recorded for each Geiger counter. The lab was active aboard the ISS for 30 days with data downlinked on average every 3 days before power was cut and the lab awaited return to Earth in June 2019.

Ground-Control

In addition to the preflight growth test and on-orbit negative control, Earth-based growth experiments were performed postflight, replicating the conditions of the flight-experiment without radiation. The same methods and techniques were utilized when preparing the cultures on solid medium. A time-dependent temperature profile analogous to the on-orbit experiment was replicated and collection of graphical data was performed in the same intervals to record the growth behavior.

Evaluation of Growth

Photographs of the cultures were processed with MATLAB³⁹ to derive the average brightness values for congruent subsections of each image (cf. supplementary material 1, section C and figure S2), as proxy for biomass formation. These average brightness values were then normalized so as to render the relative optical density (OD) ranging from zero to one (cf. supplementary material 2) over time. With exponential regression, this allowed growth rates “ k ” to be determined. Based on these, a relative difference between k_{exp} for the on-orbit experiment and the ground-control, k_{ctrl} , was estimated.

Evaluation of On-Orbit Radiation

Cumulative radiation counts, derived from the counts recorded by the Geiger counters of control- and fungus-side throughout the course of the on-orbit experiment, were plotted over time. The relative difference in radiation attenuation (in percent) between negative-control and fungus-side was determined based on the slope of linear regressions in different phases, which were defined based on the relative OD. Phase 1, the initial phase, was defined for a relative OD below 5% of the maximum, corresponding to the first 10 h. Phase 2, the growth phase, was defined for a relative OD between 5% and 95% of the maximum, correspondingly starting 10 h after the start (t_0), and ending 60 h after t_0 . Phase 3, the stationary phase, includes the remaining data from 60 – 718 h after t_0 , accordingly corresponding to a relative OD greater than 95% of the total maximum.

Further, total radiation was quantified in dose equivalents, with an estimate correlation between counts-per-minute (CPM) and radiation dose for the PocketGeiger Type5 of $4 \text{ CPM} \approx 0.075 \pm 0.025 \mu\text{Sv/h}$ ⁴⁰, based on the total cumulative recorded counts over the 30 day runtime of the experiment (cf. supplementary material 2).

Radiation Attenuation Analysis

Applying Lambert's law, the concept of linear attenuation served to evaluate the experimental data, under the assumption that no alpha- and beta-particles could reach the experiment, as neither would be able to penetrate the hull of the ISS⁴¹. Focusing on ionizing electromagnetic radiation, the analysis determined the attenuation capacity of the fungal biomass within the absorption spectrum of the employed Geiger counters (cf. supplementary material 1, section B & D).

To interpret the results in light of a more relevant (real-world / Space radiation environment) scenario, experimental findings were used to inform a theoretical analysis. This relied on the extensive resources that exist for attenuation coefficients of different materials (and mixtures thereof) over a range of photon energies by means of the NIST X-ray Attenuation Databases⁴². Particularly, MACs for the respective compounds and mixtures (cf. supplementary material 3) were derived from NIST-XCOM for total coherent scattering. The non-linear influence of secondary radiation was respected by means of buildup-factors⁴³ and equivalent kinetic energies of subatomic and elementary particles in electronvolts (eV) were used in the calculations. The correlations and assumptions, as well as the specific workflow used in the attenuation analyses are described in detail in supplementary material 1, section D & E.

Results & Discussion

Pre-Flight - Cold-Stow Growth-Test

The 'Cold-Stow' experiment showed that for all refrigerated sample-plates there was insignificant fungal growth immediately upon removal from incubation at 4°C (no fungal growth prior to t_0) for all trialed timeframes. Furthermore, all samples exhibited similar growth once at ambient temperature, regardless of the time spent in cold storage.

Growth Advantage On-Orbit

From the point the hardware was powered on aboard the ISS, the temperature rose sharply from the initial 22°C, reaching 30°C within 4 hours and stabilized after 8 hours around $31.5 \pm 2.4^\circ\text{C}$ for the rest of the experiment (cf. supplementary material 2).

Many dimorphic fungi are characterized by slow growth and require up to 14 days for significant biomass formation to occur at an optimum temperature around 25°C⁴⁴. In the on-orbit lab, *C. sphaerospermum* reached maximum growth already after 2 days, as discernible from the photographic data (cf. supplementary material 1, figure S2) and derived growth curves, shown in figure 2. Comparison with the ground-controls indicates that the fungus experienced faster-than-normal growth aboard the ISS. In respect to the two separate control experiments, the growth rate in the on-orbit experiment was 1.2-fold higher (based on $k_{flight} = 0.194 \text{ h}^{-1}$ and $k_{ground} = 0.161 \text{ h}^{-1}$, determined for the on-orbit experiment and ground-control average, respectively, as per the data shown in figure 2B). It is further worth mentioning, that in preliminary ground-control experiments often poor growth was observed at 30°C, as compared to RT (data not shown), with only sporadic coverage of the PDA with fungal colonies (cf. supplementary material 1, figure S3). The inconsistency in growth among the ground-controls is also reflected by the rather large deviations between the individual replicates of the two

experiments depicted in figure 2 (as per the error bars representing standard deviation). However, in no case growth higher than in the on-orbit experiment was observed (cf. raw data in supplementary material 2). The observation that higher than optimum incubation temperatures rapidly hindered growth, as has been reported before⁴⁵, further strengthens the conclusion that the Space environment benefited the fungus.

The growth advantage in Space may be attributable to the utilization of ionizing radiation of the Space environment by the fungus as a metabolic support function, as has been reported for other high-radiation environments: it has previously been shown that *C. sphaerospermum* can experience up to three times faster growth than normal with gamma-rays 500 times as intense as normal^{28,46}^[1].

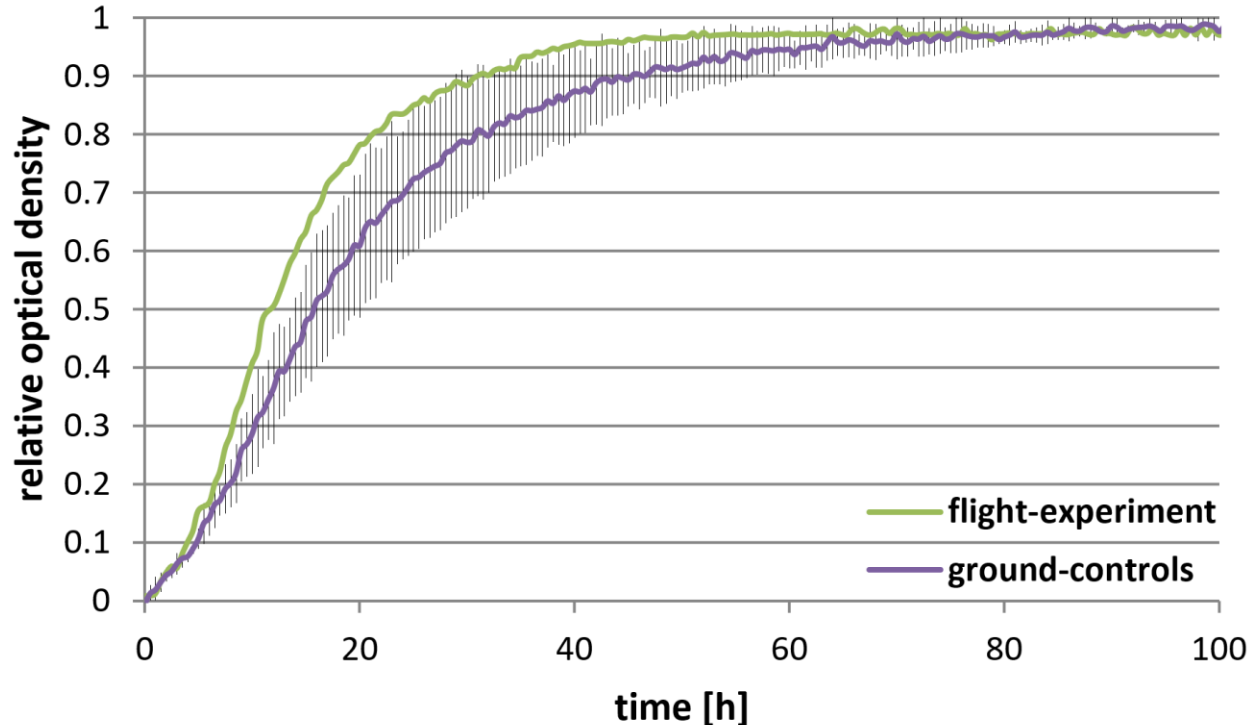


Figure 2: Growth curves (initial 100 h shown) for *C. sphaerospermum* on PDA, depicted by means of connected data-points of relative optical densities. The curves were consolidated to t_0 as the onset of exponential growth. While the on-orbit experiment (green) was a single run, the ground-control growth-experiment (purple) was conducted three times (two replicates in each of the three runs). The error bars show the standard deviation between the three separate runs.

Radiation Attenuation On-Orbit

Given the specific absorption range of the radiation-sensor (cf. supplementary material 1, section B), the observed radiation levels were within the expected range for LEO. Independent of the absolute radiation levels, only the relative difference in ionizing events recorded beneath each side of the Petri dish was significant for the experiment (congruence of the radiation sensors had been ensured before flight,

¹ Measured by the dose equivalent, which is 144 mSv/a⁸ for the ISS and 2.4 – 6.2 mSv for Earth^{7,47}. The radiation on the ISS is about 20 - 60 times stronger than the average background on Earth, however 80% of this is attributable to GCR, which is mostly composed of particle radiation. Hence the fraction of (gamma-) radiation utilizable by the fungus may not be equivalently significant.

data not shown). The radiation levels directly beneath the side of the Petri dish inoculated with *C. sphaerospermum* decreased throughout the experiment (as compared to the negative-control), particularly correlating with biomass formation: while there was no significant difference over the first 12 – 24 h, a constant attenuation was observable in the later stage of the experiment (cf. figure 3). While no further gain in optical density was observed past two days into the experiment (cf. figure 2), the mark of 240 h onward was chosen to determine the attenuation capacity, in order to be conservative. This allowed an additional eight days of maturation before fungal growth was considered complete and melanin content to be constant. The linearity of the trendlines (figure 3B) supports this conclusion. The full dataset and additional plots of the complete radiation data over the whole course of the experiment can be found in supplementary material 2.

The periodic, slight fluctuations of the radiation, especially recognizable in figure 3A, may be explainable with the orbit time / position of the ISS relative to celestial bodies and orientation of the experiment especially in respect to the sun (either towards or facing away from it). This is supported by the observation that these fluctuations coincide for the recordings of both Geiger counters throughout the entire experiment. For single spikes (as particularly prominent in the incremental plot of radiation events in supplementary material 2), solar events (flare / particle event) are also plausible explanations.

Over the first 24 h of the experimental trial, radiation levels beneath the fungal-growth side of the Petri dish were by average only 0.5% lower. Towards the end of the experiment, an almost 5-fold increase in radiation attenuation could be observed relative to the control side, with average radiation levels 2.42% lower than those of the negative-control (as per the difference of the trendlines' slopes given in figure 3). This shows a direct relationship between the amount of fungal biomass (and putatively the melanin content thereof) and the dissipated ionizing radiation. With a baseline difference between the two sensors of 0.5% (considering that the fungus may have contributed to this), the observed radiation attenuating capacity can be stated as $2.17 \pm 0.25\%$. Since radiation is ubiquitous in Space and only one side of the Geiger counter was shielded by the fungus, it is postulated that only half of the radiation was blocked. Therefore, it can be extrapolated that the fungus would reduce total radiation levels (of the measured spectrum) by $4.34 \pm 0.5\%$ were it fully surrounding an object. Considering the thin fungal lawn, this shows the significant ability of *C. sphaerospermum* to shield against space radiation.

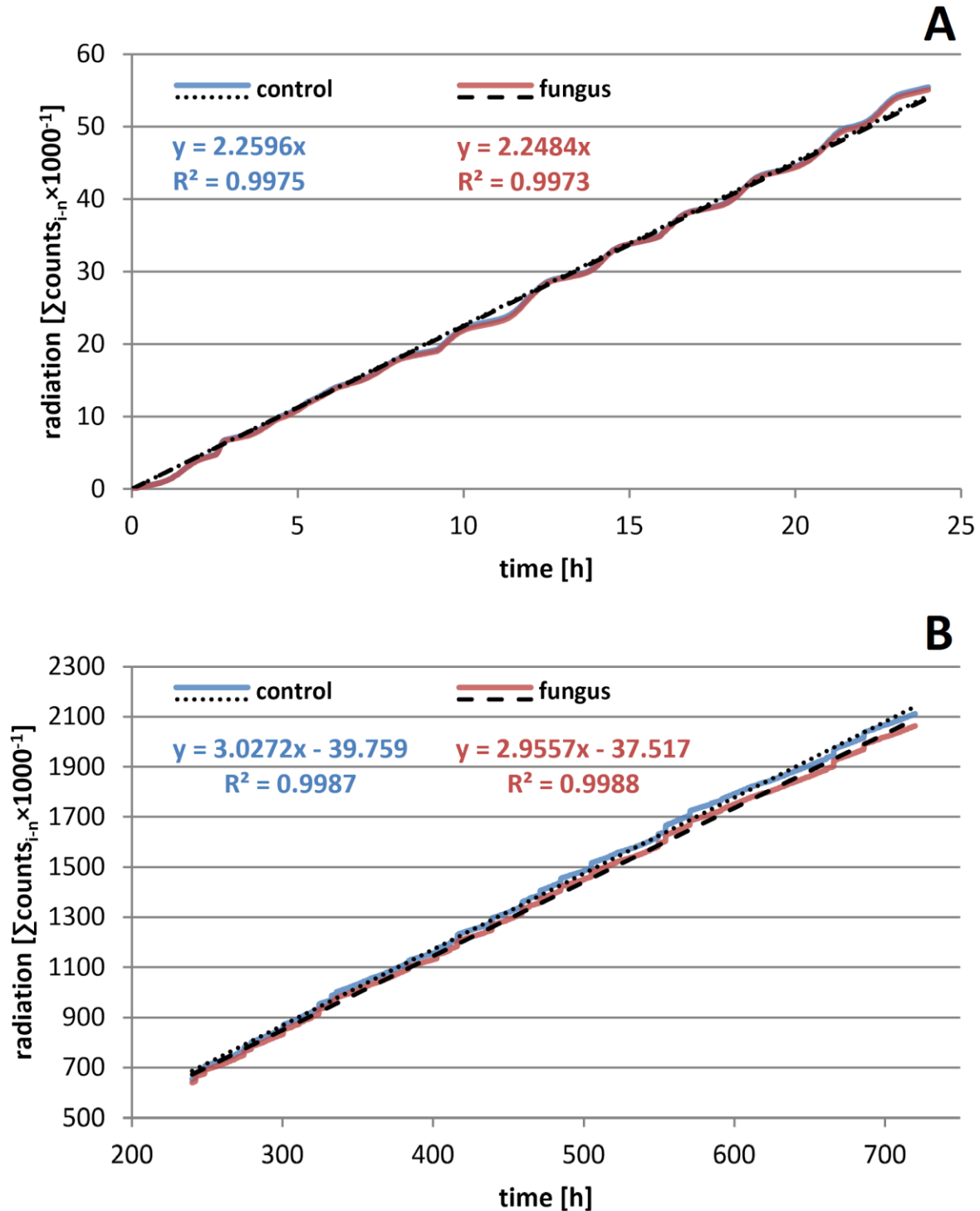


Figure 3 A & B: Cumulative radiation counts of the control and the fungus over time. A: initial phase (0 – 24 h), B: final $\frac{2}{3}$ of the experiment (240 – 718 h). For the sake of legitimacy, the cumulative count of ionizing events (radiation) was scaled-down three orders of magnitude ($\times 1000^{-1}$). While in section ‘A’ the regression lines almost coincide, a significant difference in the slope is evident in section ‘B’ (where the fungus was fully matured), corresponding to an attenuation of the transmitted radiation.

Radiation Attenuation in Light of ISRU on Mars

The average rates of ionizing events over the whole course of the experiment were 48.9 and 47.8 CPM for the negative-control and the fungus-side, respectively (cf. supplementary material 2). Based on these numbers, dose equivalents of 0.916 $\mu\text{Sv/h}$ and 0.872 $\mu\text{Sv/h}$ were estimated. These, together with a maximum thickness of 1.67 mm of the fungal lawn, were the primary figures used in the attenuation analysis. The linear attenuation coefficient (LAC) of *C. sphaerospermum*, μ_{Fungus} , provides a measure for the fungus' capacity to shield against ionizing radiation and further allowed the estimation of the biomass' melanin content. From this, the thickness of melanized fungus that could negate a certain radiation dose equivalent was approximated, to put the shielding potential into perspective. Relevant calculations can be found in supplementary material 1, section D & E.

The LAC of *C. sphaerospermum* at 10 keV was determined to be $\mu_{\text{Fungus}} = 10.5 \pm 5.9 \text{ cm}^{-1}$, and with a density of $\rho_m \approx 1.1 \text{ g/cm}^3$ for wet microbial biomass⁴⁸ the MAC for the fungus was derived as $\mu_{\text{Fungus}}/\rho_m = 9.51 \text{ cm}^2/\text{g}$. The experimental attenuation coefficient is, however, only valid for the specific gamma-energy absorption range of the employed Geiger counters ($\sim 10 \text{ keV}$, cf. supplementary material 1, section B). An approximate LAC for melanized biomass at any energy can be determined if the composition of fungal biomass, in particular the melanin content, is known. Here, it was estimated that about 8.6% [$w_{\text{melanin}}/w_{\text{CDW}}$] of the accumulated *C. sphaerospermum* biomass were composed of melanin (cf. supplementary material 1, section D for derivation).^[2] The high melanin content of *C. sphaerospermum* is potentially a metabolic response to the strong radiation environment of the ISS, analogous to other studies on the fungus in ionizing environments.

Based on the empirical elemental formula for fungal biomass⁵¹ and the water content of fungus microorganisms⁴⁹ the theoretical MAC of melanized fungal biomass at 150 MeV (the average cumulative energy of the Martian radiation environment)⁵² was determined (cf. supplementary material 3). This allowed μ_{Fungus} and the shielding potential of melanized biomass to be compared in a deep Space environment equivalent scenario to other (theoretical) attenuation capacities of common aerospace construction materials and those considered for passive shielding against Space radiation (cf. table S1, supplementary material 1). Both forms of the pigment that are common in melanized fungi (eumelanin and DHN-melanin) are comparatively effective radiation attenuators ($\mu_{\text{Melanin}} = 0.046 \text{ cm}^{-1}$ at 150 MeV). Therefore, the predicted high attenuation capacity of melanized fungi at 150 MeV ($\mu_{\text{Fungus}} = 0.023 \text{ cm}^{-1}$, compared to non-melanized fungal biomass with $\mu_{\text{Biomass}} = 0.016 \text{ cm}^{-1}$) is a result of the high LAC of melanin.

Materials with large LACs typically have high densities and are therefore heavy (like e.g. steel, cf. supplementary material 3). *C. sphaerospermum*, however, just like melanin, has a comparatively (for organic compounds) large innate LAC and a low density, which is desirable in aerospace. Unlike steel or aluminum, melanin may be available from ISRU through biotechnology. Due to the saprotrophic nature of the fungus, it grows on virtually any carbon-based biomass, which on Mars could for instance be cyanobacterial lysate (as previously proposed⁵³) and/or organic waste. The nature of radiotrophic fungi also makes them inevitably/necessarily radioresistant, and thus effectively a self-regenerating and -replicating radiation shield. As biomass has large water content, the fungus may pose an excellent passive radiation shield for GCR in particular.

² The melanin content of 8.6% [$w_{\text{melanin}}/w_{\text{CDW}}$] for wet biomass is approx. equivalent to 21.5% [$w_{\text{melanin}}/w_{\text{CDW}}$] for dry biomass (based on 60% water content⁴⁹), which seems realistic in lieu of reported values for microscopic fungi of 11.2%³⁷ and 31.5%⁵⁰ [$w_{\text{melanin}}/w_{\text{CDW}}$].

Regardless of how effective a radiation attenuator may be, passive radiation shielding is ultimately always limited by mass ¹⁰. To increase the density and thus the LAC, fungal biomass or melanin itself could be integrated with *in-situ* resources that are abundant at destination, such as regolith. In a case study we estimated that a ~ 2.3 m layer of melanized fungal biomass (8.6% [$w_{\text{melanin}}/w_{\text{CWW}}$] melanin-content) would be needed to lower Martian radiation levels to those on Earth (from 234 mSv/a to 6.2 mSv/a) ^{52,7}, whereas an equimolar composite of melanin and Martian regolith would only require a ~ 1 m thick layer for the same reduction of radiation. For comparison, in case of pure Martian regolith, about 1.3-times the thickness would be required to absorb the respective dose equivalent. When conducting the same analysis with purely non-melanized fungal biomass, a thickness of ~ 3.5 m is required for the same shielding effect (reduction of radiation by 97%). Table 1 provides an overview of the inputs and outputs of this basic assessment, details can be found in supplementary material 1, section E.

Table 1: Comparison of radiation attenuating capacity of *in-situ* resources on Mars with melanized composites. Attenuation coefficients for the compounds were obtained from the NIST XCOM database ⁴², with buildup-factors generated by the RadPro Calculator ⁵⁴, based on molecular formulas and/or densities for the respective materials as referenced, unless trivial or noted otherwise.

| Material and literature source for molecular formula and density | Mass Attenuation Coefficient 'μ/ρ' [cm^2/g] at 150 MeV * | Linear Attenuation Coefficient 'μ' [cm^{-1}] at relative material density | Required thickness [cm] to reduce Martian radiation levels by ~ 97% [§] |
|---|--|---|---|
| Water | 0.0149 | 0.0149 | 367 |
| Martian regolith ⁵⁵ | 0.0268 | 0.0407 | 128 |
| Martian regolith + melanin (equimolar mixture) ⁵⁶ | 0.0288 | 0.0518 | 106 |
| Non-melanised fungus ^{§ 51} | 0.0141 | 0.0155 | 351 |
| Melanized fungus [#] | 0.0213 | 0.0234 | 232 |

* cumulative radiation environment on the surface of Mars ⁵²; [§] from 234 mSv/a, the average radiation dose on Mars ⁵², to 6.2 mSv/a the average radiation dose on Earth ⁷; [§] based on an empirical elemental formula for the biomass of baker's yeast ⁵⁷, adjusted for 60% water content ⁴⁹; [#] based on 91.4% [w/w] non-melanized fungal biomass (baker's yeast ⁵⁷, adjusted for 60% water content ⁴⁹), and 8.6% [w/w] melanin content (DHN-melanin) as per supplementary material 3.

Various melanins and melanin-based composites have been explored as means to attenuate radiation, and it has been found that the overall attenuation capability can be increased in a synergistic way: the MAC curve of a melanin-bismuth composite, for instance, is about double that of lead at energies in a low MeV range ⁵⁸. Another example of an enhanced, melanin-based radiation protection agent that is potentially bio-based is selenomelanin: it was found that under increased radiation, nanoparticles of the compound could efficiently protect cells against cell cycle changes ⁵⁹. In future, blends or layers of melanin with other materials, analogous to the concept of Martian 'biolith' ⁶⁰, may yield composites that more efficiently shield against cosmic rays. Advanced additive manufacturing technologies such as 3D bioprinting, may ultimately also allow the creation of smart 'living composite'

materials that are adaptive, self-healing and largely autonomous⁶¹. This will, however, require extensive further theoretical as well as experimental studies. Section G in supplementary material 1 contains additional remarks on this topic.

Conclusion

Through the design of a subtle yet simple experimental setup, implemented as a small single payload, it could be shown that the melanized fungus *C. sphaerospermum* can be cultivated in LEO, while subject to the unique microgravity and radiation environment of the ISS. Growth characteristics further suggested that the fungus not only adapts to but thrives on and shields against Space radiation, analogous to Earth-based studies. It was found that a microbial lawn of less than 2 mm thickness already decreased the measured radiation levels by at least 1.92% and potentially up to 4.84%. Attenuation of radiation was consistent over the whole course of the 30-day experiment, allowing a scenario-specific linear attenuation coefficient for *C. sphaerospermum* to be determined. This was further used to approximate the melanin content of the biomass, which corresponded well with literature, serving to explain the significant reduction in radiation levels by the fungal lawn. Based on the melanin content, the theoretical radiation attenuation capacity of melanized fungal biomass could be put into perspective at constant equivalent ionizing radiation energy levels resembling deep-space conditions: melanized biomass and melanin containing composites were ranked effective radiation attenuators, emphasizing the great potential melanin holds as component of radiation shields to protect from Space radiation.

Being a living organism, *C. sphaerospermum* self-replicates from microscopic amounts, which opens the door for ISRU through biotechnology and significant savings in up-mass. Often nature has already developed blindly obvious yet surprisingly effective solutions to engineering and design problems faced as humankind evolves - *C. sphaerospermum* and melanin could thus prove to be invaluable in providing adequate protection of explorers on future missions to the Moon, Mars and beyond.

Acknowledgments

As members of ‘Team Orion’ Srikar Kaligotla, Finn Poulin, and Jamison Fuller were instrumental for the conception and planning of the experiment. We cordially extend our thanks to the Higher Orbits Foundation for providing funding for this project through the ‘Go For Launch!’ program, and to Space Tango, for the technical solution, logistics, and implementation of the experiment.

The team would like to specifically express deep gratitude to Michelle Lucas of Higher Orbits, for her guidance and enthusiastic encouragement and to Matthew Clobridge of the Durham County Public Library for bringing the program into reach for the team in the first place, as well as to Gentry Barnett of Space Tango. We would also like to thank Dr. Robert Gotwals for his guidance on the scientific process, and Dr. Jonathan Bennet, who introduced the team to calculations used to interpret the results.

We want to make known our appreciation for our colleagues who supported the research every step of the way and provided encouragement throughout the composition of the manuscript. Finally, we wish to thank our families and friends for their support and encouragement throughout this study.

Author contributions

GKS and XG, in conjunction with colleagues Srikar Kaligotla, Finn Poulin, and Jamison Fuller, conceived of the idea for the study in 2018 and composed the proposal for funding. GKS wrote the initial draft of this paper with support from XG. NJHA joined the team in early 2020, re-visiting and analyzing the data, revised and refined the manuscript. All authors have read and approved the final version of the manuscript. The authors declare no competing interests.

References

1. NASA Artemis. <https://www.nasa.gov/specials/artemis/> (2020).
2. Loff, S. Moon to Mars. NASA <http://www.nasa.gov/topics/moon-to-mars> (2018).
3. Drake, B. G. & Watts, K. D. Human Exploration of Mars Design Reference Architecture 5.0 Addendum #2. 598.
4. Gruenwald, J. Human outposts on Mars: engineering and scientific lessons learned from history. *CEAS Space J.* **6**, 73–77 (2014).
5. Cucinotta, F. A., Kim, M.-H. Y. & Chappell, L. J. Space Radiation Cancer Risk Projections and Uncertainties – 2012. 186 (2012).
6. Afshinnekoo, E. *et al.* Fundamental Biological Features of Spaceflight: Advancing the Field to Enable Deep-Space Exploration. *Cell* **183**, 1162–1184 (2020).
7. ANS / Public Information / Resources / Radiation Dose Calculator. <https://ans.org/pi/resources/dosechart/msv.php> (2020).
8. Cucinotta, F. A., Kim, M.-H. Y., Willingham, V. & George, K. A. Physical and Biological Organ Dosimetry Analysis for International Space Station Astronauts. *Radiat. Res.* **170**, 127–138 (2008).
9. Letaw, J. R., Silberberg, R. & Tsao, C. H. Galactic Cosmic Radiation Doses to Astronauts Outside the Magnetosphere. in *Terrestrial Space Radiation and Its Biological Effects* (eds. McCormack, P. D., Swenberg, C. E. & Bueker, H.) 663–673 (Springer US, 1988). doi:10.1007/978-1-4613-1567-4_46.
10. Chancellor, J. C. *et al.* Limitations in predicting the space radiation health risk for exploration astronauts. *Npj Microgravity* **4**, 1–11 (2018).
11. Spedding, C. P., Nuttall, W. J. & Lim, S. Energy requirements of a thermally processed ISRU radiation shield for a lunar habitat. *Adv. Space Res.* **65**, 2467–2474 (2020).
12. McCaffrey, J. P., Shen, H., Downton, B. & Mainegra-Hing, E. Radiation attenuation by lead and nonlead materials used in radiation shielding garments. *Med. Phys.* **34**, 530–537 (2007).
13. Ambroglini, F., Battiston, R. & Burger, W. J. Evaluation of Superconducting Magnet Shield Configurations for Long Duration Manned Space Missions. *Front. Oncol.* **6**, (2016).
14. Hall, L. In-Situ Resource Utilization. NASA <http://www.nasa.gov/isru> (2017).
15. Rothschild, L. J. Synthetic biology meets bioprinting: enabling technologies for humans on Mars (and Earth). *Biochem. Soc. Trans.* **44**, 1158–1164 (2016).
16. Menezes, A. A., Cumbers, J., Hogan, J. A. & Arkin, A. P. Towards synthetic biological approaches to resource utilization on space missions. *J. R. Soc. Interface* **12**, 20140715 (2015).
17. Berliner, A. *et al.* Towards a Biomanufacturing on Mars. (2020) doi:10.20944/preprints202012.0714.v1.
18. Nangle, S. N. *et al.* The case for biotech on Mars. *Nat. Biotechnol.* **38**, 401–407 (2020).
19. Cockell, C. S. *et al.* Space station biomineralization experiment demonstrates rare earth element extraction in microgravity and Mars gravity. *Nat. Commun.* **11**, 5523 (2020).
20. Aversch, N. J. H. & Rothschild, L. J. Metabolic engineering of *Bacillus subtilis* for production of *para*-aminobenzoic acid – unexpected importance of carbon source is an advantage for space application. *Microb. Biotechnol.* **12**, 703–714 (2019).
21. Nov 1, S. C. / P. & 2019. Biological pigment that acts as nature’s sunscreen set for space journey. *The Hub* <https://hub.jhu.edu/2019/11/01/melanin-space-study/> (2019).
22. Cordero, R. J. B. Melanin for space travel radioprotection. *Environ. Microbiol.* **19**, 2529–2532 (2017).
23. Kalawate, A. & Mehetre, S. Isolation and characterization of mold fungi and insects infecting sawmill wood, and their inhibition by gamma radiation. *Radiat. Phys. Chem.* **117**, (2015).
24. Krisko, A. & Radman, M. Biology of Extreme Radiation Resistance: The Way of *Deinococcus radiodurans*. *Cold Spring Harb. Perspect. Biol.* **5**, (2013).
25. Eisenman, H. C. & Casadevall, A. Synthesis and assembly of fungal melanin. *Appl. Microbiol. Biotechnol.* **93**, 931–940 (2012).
26. Zhdanova, N. N., Tugay, T., Dighton, J., Zheltonozhsky, V. & Mcdermott, P. Ionizing radiation attracts soil fungi. *Mycol. Res.* **108**, 1089–1096 (2004).
27. Dadachova, E. & Casadevall, A. Ionizing Radiation: how fungi cope, adapt, and exploit with the help of melanin. *Curr. Opin. Microbiol.* **11**, 525–531 (2008).
28. Dadachova, E. *et al.* Ionizing Radiation Changes the Electronic Properties of Melanin and Enhances the Growth of Melanized Fungi. *PLOS ONE* **2**, e457

- (2007).
29. Méndez-Vilas, A. *Current Research, Technology and Education Topics in Applied Microbiology and Microbial Biotechnology*. (Formatex Research Center, 2010).
 30. Cortesão, M. *et al.* *Aspergillus niger* Spores Are Highly Resistant to Space Radiation. *Front. Microbiol.* **11**, (2020).
 31. Schweitzer, A. D. *et al.* Physico-Chemical Evaluation of Rationally Designed Melanins as Novel Nature-Inspired Radioprotectors. *PLOS ONE* **4**, e7229 (2009).
 32. Pacelli, C. *et al.* Melanin is effective in protecting fast and slow growing fungi from various types of ionizing radiation. *Environ. Microbiol.* **19**, 1612–1624 (2017).
 33. Verseux, C. *et al.* Sustainable life support on Mars – the potential roles of cyanobacteria. *Int. J. Astrobiol.* **15**, 65–92 (2016).
 34. X-Ray Mass Attenuation Coefficients. *NIST* <https://www.nist.gov/pml/x-ray-mass-attenuation-coefficients> (2009).
 35. Ledford, H. Hungry fungi chomp on radiation. *Nature* (2007) doi:10.1038/news070521-5.
 36. Space Tango, Inc. <https://www.issnationallab.org/implementation-partners/space-tango-inc> (2020).
 37. Baldwin, W. W. & Kubitschek, H. E. Buoyant density variation during the cell cycle of *Saccharomyces cerevisiae*. *J. Bacteriol.* **158**, 701–704 (1984).
 38. Space Tango | TangoLab. *Space Tango* <https://spacetango.com/tangolab/> (2020).
 39. Read and Analyze Image Files - MATLAB & Simulink. https://www.mathworks.com/help/matlab/import_export/read-and-analyze-image-files.html (2020).
 40. Pocket Geiger Radiation Sensor - Type 5 - SEN-14209 - SparkFun Electronics. <https://www.sparkfun.com/products/14209> (2020).
 41. NRC: Radiation Basics. <https://www.nrc.gov/about-nrc/radiation/health-effects/radiation-basics.html> (2020).
 42. XCOM: Photon Cross Sections Database. *NIST* <https://www.nist.gov/pml/xcom-photon-cross-sections-database> (2009).
 43. SHIMIZU, A., ONDA, T. & SAKAMOTO, Y. Calculation of Gamma-Ray Buildup Factors up to Depths of 100 mfp by the Method of Invariant Embedding, (III). *J. Nucl. Sci. Technol.* **41**, 413–424 (2004).
 44. Bosshard, P. P. Incubation of fungal cultures: how long is long enough? *Mycoses* **54**, e539-545 (2011).
 45. Zalar, P. *et al.* Phylogeny and ecology of the ubiquitous saprobe *Cladosporium sphaerospermum*, with descriptions of seven new species from hypersaline environments. *Stud. Mycol.* **58**, 157–183 (2007).
 46. Castelveccchi, D. Dark power: Pigment seems to put radiation to good use. *Sci. News* **171**, 325–325 (2007).
 47. Rühm, W. *et al.* Typical doses and dose rates in studies pertinent to radiation risk inference at low doses and low dose rates. *J. Radiat. Res. (Tokyo)* **59**, ii1–ii10 (2018).
 48. Bakken, L. R. & Olsen, R. A. Buoyant Densities and Dry-Matter Contents of Microorganisms: Conversion of a Measured Biovolume into Biomass. *Appl. Environ. Microbiol.* **45**, 1188 (1983).
 49. Fraction of cell mass that is water - Budding yeast *Saccharomyces cerevisiae* - BNID 103689. <https://bionumbers.hms.harvard.edu/bionumber.aspx?id=103689> (2020).
 50. Fraction of cell wall out of total cell mass - Budding yeast *Saccharomyces cerevisiae* - BNID 104592. <https://bionumbers.hms.harvard.edu/bionumber.aspx?id=104592> (2020).
 51. Battley, E. H. An empirical method for estimating the entropy of formation and the absolute entropy of dried microbial biomass for use in studies on the thermodynamics of microbial growth. *Thermochim. Acta* **326**, 7–15 (1999).
 52. Hassler, D. M. *et al.* Mars' Surface Radiation Environment Measured with the Mars Science Laboratory's Curiosity Rover. *Science* **343**, (2014).
 53. Billi, D., Fernandez, B. G., Fagliarone, C., Chiavarini, S. & Rothschild, L. J. Exploiting a perchlorate-tolerant desert cyanobacterium to support bacterial growth for *in situ* resource utilization on Mars. *Int. J. Astrobiol.* **20**, 29–35 (2021).
 54. Rad Pro Calculator: Online Nuclear Calculations and Free Health Physics Software. <http://www.radprocalculator.com/> (2020).
 55. Foley, C. N., Economou, T. & Clayton, R. N. Final chemical results from the Mars Pathfinder alpha proton X-ray spectrometer. *J. Geophys. Res. Planets* **108**, (2003).

56. PubChem. Melanin.
<https://pubchem.ncbi.nlm.nih.gov/compound/6325610> (2020).
57. Fraction of Cell wall out of total cell weight - Budding yeast *Saccharomyces cerevisiae* - BNID 104588.
<https://bionumbers.hms.harvard.edu/bionumber.aspx?id=104588> (2020).
58. El-Bialy, H. A., El-Gamal, M. S., Elsayed, M. A., Saudi, H. A. & Khalifa, M. A. Microbial melanin physiology under stress conditions and gamma radiation protection studies. *Radiat. Phys. Chem.* **162**, 178–186 (2019).
59. Cao, W. *et al.* Selenomelanin: An Abiotic Selenium Analogue of Pheomelanin. *J. Am. Chem. Soc.* (2020) doi:10.1021/jacs.0c05573.
60. Shiwei, N., Dritsas, S. & Fernandez, J. G. Martian biolith: A bioinspired regolith composite for closed-loop extraterrestrial manufacturing. *PLOS ONE* **15**, e0238606 (2020).